Studying gene expression scaling with cell size in *Arabidopsis thaliana*: the role of the nuclear RNA exosome complex

Emily Tåhlin

Examensarbete/Självständigt arbete • 15 hp
Sveriges lantbruksuniversitet, SLU
Department of plant biology
Uppsala 2023

Emily Tåhlin

Handledare: Stefanie Rosa, SLU, Department of Plant Biology
Bitr. handledare: Alejandro Fonseca Cardenas, SLU, Department of Plant Biology
Examinator Jens Sundström, SLU, Department of Plant Biology

Omfattning: 15hp
Nivå och fördjupning: Grundnivå, G2E
Kurstitel: Självständigt arbete i biologi, G2E
Kurskod: EX0894
Program/utbildning: Biologi, 180hp
Part number: 204

Publishing and archiving

Approved students' theses at SLU are published electronically. As a student, you have the copyright to your own work and need to approve the electronic publishing. If you check the box for YES, the full text (pdf file) and metadata will be visible and searchable online. If you check the box for NO, only the metadata and the abstract will be visible and searchable online. Nevertheless, when the document is uploaded it will still be archived as a digital file. If you are more than one author, the checked box will be applied to all authors. You will find a link to SLU's publishing agreement here:

- https://libanswers.slu.se/en/faq/228318.

☒ YES, I/we hereby give permission to publish the present thesis in accordance with the SLU agreement regarding the transfer of the right to publish a work.

☐ NO, I/we do not give permission to publish the present work. The work will still be archived and its metadata and abstract will be visible and searchable.

Table of contents

1: Acknowledgements

I want to thank my supervisors Stefanie Rosa and Alejandro Fonseca Cardenas for your immensely valuable feedback and mentorship along the way. I also want to thank all members of The Rosa Lab for discussions and feedback.

2: Abstract

The scaling of organ size with body size - known as morphological allometry - is a fundamental mechanism observed in all organisms (Mirth *et al*. 2016). Scaling mechanisms have also been shown at a cellular level, with mRNA levels linearly scaling with cell size, but knowledge about the cellular processes controlling it has been limited (Berry *et al*. 2022). However, recent evidence in human cells suggest that nuclear mRNA transcripts - through a negative feedback mechanism - inhibit transcription of Pol II, so that Pol II concentrations remain constant in relation to cell size (Berry *et al*. 2022b). Here, we applied this hypothesis to plants by studying how transcription scaling was affected by mutations disrupting the nuclear RNA exosome complex in *A. thaliana*. We performed smFISH, and compared the mutants *hen2-4* and *rrp4-2* with Col-0. We found that the mutants accumulated more transcripts with increasing cell size than WT, but remarkably, the increased number of transcripts in the mutants were found in the cytoplasm and not in the nucleus. This suggests that loss of nuclear exosome functionality - meaning decreased mRNA decay - results in an increased nuclear mRNA export. This could mean that the cell is trying to minimize nuclear transcript accumulation to prevent inhibition of synthesis of new mRNAs, indicating that a negative feedback of nuclear mRNA is also operating in plants.

Key words: RNA, transcription, cell size, smFISH, *Arabidopsis thaliana*.

3: Introduction

Despite different environmental conditions, individuals have the ability to regulate morphological traits to match final body size, meaning there is a relationship between shape and size (Mirth *et al*. 2016). This is known as morphological allometry, and describes the scaling of organ size with body size. A similar mechanism has been observed at a cellular level, with mRNA transcripts linearly scaling with cell size (Berry *et al*. 2022). This is pivotal for cell viability for several reasons: First of all, larger cells require more material to maintain macromolecule concentrations so that core cellular processes can proceed (Berry *et al*. 2022a). In addition, during the cell cycle, cells grow before dividing, and maintaining mRNA homeostasis during this growth is crucial (Vargas-Garcia *et al*. 2018). Despite the fundamentality of gene expression cell size scaling, the regulatory cellular processes controlling it have until recently remained unknown. However, with increasing interest for the subject in the field, and the development of methods such as Single-molecule RNA fluorescence *in situ* hybridization (smFISH), in combination with cell size quantification, we are now beginning to understand some mechanisms involved in this big cellular machinery (Berry *et al*. 2022a).

One model that has been presented is the “Limiting factor model”. In this model, a specific factor that is essential for transcription has a constant concentration that is exactly coordinated with cell size (Berry *et al*. 2022a). There is evidence in both human cells and the yeasts S. *Pombe* and S. *cerevisiae* that the limiting factor could be the RNA polymerase Pol II enzyme, which is fundamental for transcription. In a study published in 2020, Sun *et al*. showed that during the cell cycle, when the size of *S. Pombe* cells increased, the amount of Pol II associated with chromatin also increased (Sun *et al*. 2020). The concentration of Pol II in the cell did not change, however increasing cell size was accompanied by a rapid import of Pol II into the nucleus, with an amount proportional to the nuclear size. In human cells, the amount of Pol II has been proven to increase both with cell and nuclear size (Berry *et al*. 2022b).

If the theory about Pol II being the limiting factor is correct, the control of its activity is of high importance since the risk of positive feedback otherwise could lead to increased

transcription of mRNAs. This includes the transcription of Pol II itself, which in turn would enhance the positive feedback even more (Berry *et al*. 2022a). Therefore, when further developing the theory of Pol II as a limiting factor, understanding the mechanisms controlling Pol II levels is essential. Several hypotheses have been presented to give clarification to this issue, with one of them being the 'mRNA based feedback model'. It has been shown in human cells that accumulation of mRNA in the nucleus - either through disruption of nuclear export or function of the exosome – leads to reduced mRNA synthesis (Berry *et al*. 2022b). It has also been found that increased mRNA levels in the nucleus lead to reduced transcriptional activity, eventually leading to lower levels of Pol II, suggesting that Pol II abundance is determined by transcriptional activity rather than the other way around. Altogether, these findings indicate that mRNA levels itself – through inhibition - control transcription in human cells and that this negative feedback mechanism enables the cell to adapt to perturbations and by doing so maintain mRNA homeostasis (Berry *et al*. 2022b).

Evidence of gene expression scaling with cell size in plants has been found in *FLOWERING LOCUS C* (*FLC*), a gene that controls flowering time (Letswaart *et al*. 2017). In a study about the kinetics of FLC and its antisense non-coding RNA – *COOLAIR* - it was discovered that mRNA levels varied greatly between cells, and that this variability was exactly linear with cell size. Strikingly, in COOLAIR-expressing cells, the size scaling of FLC was disrupted, and instead, COOLAIR transcripts scaled with cell size (Letswaart *et al*. 2017).

However, the mechanisms behind gene expression scaling with plant cell size remain unknown. The current evidence of scaling is also – to our knowledge – limited to FLC. Here, applying the leading hypothesis in other organisms of a limiting factor whose levels are controlled by negative feedback of mRNA levels, gene expression cell size scaling in *A. thaliana* was studied. Mutants of two genes associated with the nuclear exosome were evaluated: *hen2-4* and *rrp4-2* (Kamakura *et al*. 2013; Lange *et al*. 2014).

Transcripts undergo several processing steps before they become functional mRNAs, and for these steps, the exosome plays a central role (Lange *et al*. 2022). By enabling 3′-5′-exoribonuclease activities, and degrading non-functional RNAs, the nuclear exosome ensures that faulty RNAs do not get exported to the cytosol and reach ribosomes, which is crucial for cell viability (Lange *et al*. 2022).The RNA exosome is a macromolecular complex that is evolutionary conserved in all eukaryotes. Its core *Exo9* is made from the following

nine subunits: three RNA-binding proteins (RRP4, RRP40 and CS14); and six RNases (RRP41, RRP42, RRP43, RRP45, RRP46 and MTR3) (Sekorska *et al*. 2017). In *S.cerevisiae,* loss of any of these subunits is lethal, and in human cells, all nine subunits are required for maintaining exosome integrity (Allmang *et al*. 1999; Liu *et al*. 2006). HEN2 – a nucleoplasmic RNA helicase that only exists in plants - is not part of *Exo9*, however, is an important exosome co-factor involved in the processing and degradation of snoRNAs, lincRNAs and the degradation of introns and non-functional mRNAs (Western *et al*. 2002; Lange *et al*. 2014).

In this study, to evaluate the role of the nuclear exosome in transcription scaling in *A. thaliana,* we used Single-molecule RNA FISH (smFISH). SmFISH is a method that allows visualization of individual RNA molecules, and is used as a powerful tool to study transcription and gene regulation at a cellular level. By using multiple singly labeled probes (30-48 probes per target), SmFISH enables visualization of RNA molecules as discrete fluorescence spots. It was only recently developed and optimized for *A.thaliana* (Duncan et al. 2018). By following the protocol by Duncan *et al.* (Duncan *et al*. 2017), cell size scaling of *rrp4-2* and *hen2-4* mutants were studied and compared with wild type (Col-0).

4: Methods

4.1: Plant material

hen2-4, *rrp4-2* and Col-0 seeds were sterilized in 5% v/v sodium hypochlorite for 5 min and rinsed three times in sterile distilled water. After this, the seeds were stratified at 4°C for 48 h in the darkness, and then plated on Murashige and Skoog (MS) solid medium and grown in 16/8 h light/dark cycles at 22°C in vertically oriented Petri dishes. The roots were observed after 10 days of incubation.

4.2: smFISH and microscopy

To acquire fixed cells in single cell layers, ten-day-old *A.thaliana* root tips were treated with a 4% paraformaldehyde solution, and squashed on microscopic slides. These samples were then hybridized with three different probes: Exonic probes for *NIA1, PP2A* and DAPI – all with concentrations of 0,5µl/mL. For probe sequences see table 1 and 2. *PP2A* is a housekeeping gene encoding for Phosphoprotein phosphatase 2A, an enzyme crucial for cell viability, and *NIA1* encodes for a NITRATE REDUCTASE protein that participates in the first step of nitrate assimilation, when nitrate is converted into nitrite (Razavizadeh *et al*, 2018; Justyna *et al*. 2019). The used fluorophore for NIA1 was Quasar670, and Quasar570 for PP2A.

After incubating for twenty-four hours, samples were washed with a wash buffer to remove unbound probes. To minimize the presence of oxygen – which otherwise could interfere with the fluorescence – samples were incubated with a GLOX buffer, containing the enzymes glucose oxidase and bovine liver catalase. Samples were visualized with a Zeiss LSM800 inverted microscope - using an x63 oil-immersion objective – and imaged with a cooled quad-port CCD (charge-coupled device) ZEISS Axiocam 503 mono camera. For Quasar670, fluorescence was detected with a 625-655 nm wavelength excitation filter, with 665-715 nm signal detection. For Quasar570, the excitation filter was 561nm, with 570-640 nm signal detection. For DAPI, the excitation filter was 335-383 nm, with 420-470 nm signal detection. For each image, Z-steps of 0,22 µm were set to obtain sequences of optical sections. The experiment was repeated three times. However, due to technical problems, one of them was discarded, hence two of them are presented here.

4.3: Data analysis

The obtained three-dimensional images were converted into two-dimensional pictures using Cellpose, in which the cells for each two-dimensional image then were segmented (Stringer *et al.* 2020) . Finally, using Matlab and FISH quant v 3.0, the mature mRNAs for each image were quantified and assigned as nuclear or cytoplasmic transcripts depending on if they were inside or outside of the nuclear area (Mueller *et al*. 2013). Plots and statistical analyses were performed using R packages.

5: Results

To test the role of the nuclear exosome complex on transcription scaling we evaluated the number of transcripts as a function of cell size in *hen2-4* and *rrp4-2*, using smFISH probes against PP2A and NIA1 transcripts. First, linear regressions between cell area and total number of transcripts for *hen2-4*, *rrp4-2* and WT were calculated. The Pearson correlation method was used to determine the dependency between the variables (by analyzing R and p values). Logarithmic scales were used, and cells with 0 transcripts were excluded from the calculations. Next, slope comparisons between the mutants and WT were evaluated using a t-statistics between the regression models (*fig 2*). In all cases, the mutants were observed to have a more pronounced increase in the number of transcripts with increasing cell size ($P<0{,}001$), indicating that the cells cannot fully compensate for the increased accumulation of transcripts by decreasing the synthesis of new mRNAs. R values for *NIA1* were higher than *PP2A* in both *hen2-4*, *rrp4-2* and WT (*fig 4*). This was especially apparent in *hen2-4*, with the R-value for *NIA1* being R=0,389 (*fig 4, D*), compared to *PP2A* R=0,674 (*fig 2, B*). *NIA1* is known for being bursty - meaning it has a transient and rapid expression pattern that is activated by a stimulus (Alvarez *et al*. 2020). In *A.thaliana* roots, the expression of *NIA1* is mainly seen in epidermis cells of the meristem. It also expresses in vascular layers, however with a weaker expression pattern (Olas *et al*. 2019). Considering the obtained confocal pictures were snapshots - meaning they show the expression of a gene in a given time and not over time - it is expected from a bursty gene like NIA1 that in the moment when the cells are fixed, some cells might have a higher expression than others. There is also a possibility that part of the explanation is biological, meaning what we see is a phenotype specific for the studied mutants.

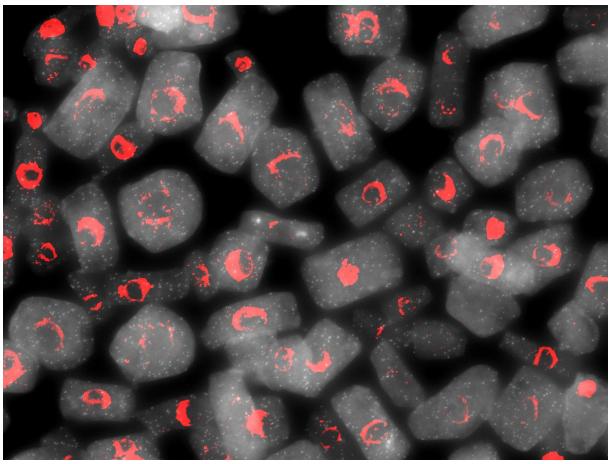

Col-0, PP2A

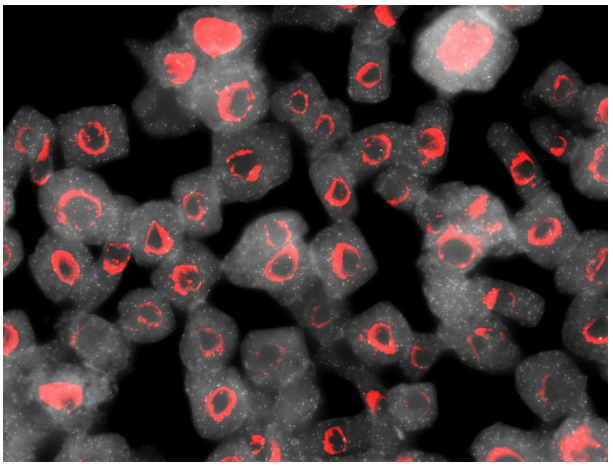

rrp4-2, PP2A

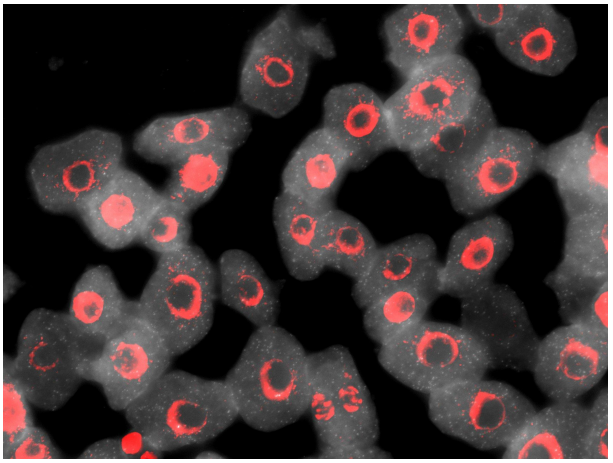

hen2-4, PP2A

Figure 1. Representative pictures of smFISH carried out on *hen2-4/rrp4-2* mutants and WT, showing PP2A mRNA (magenta) and DAPI (red). Scale bars, 20µm.

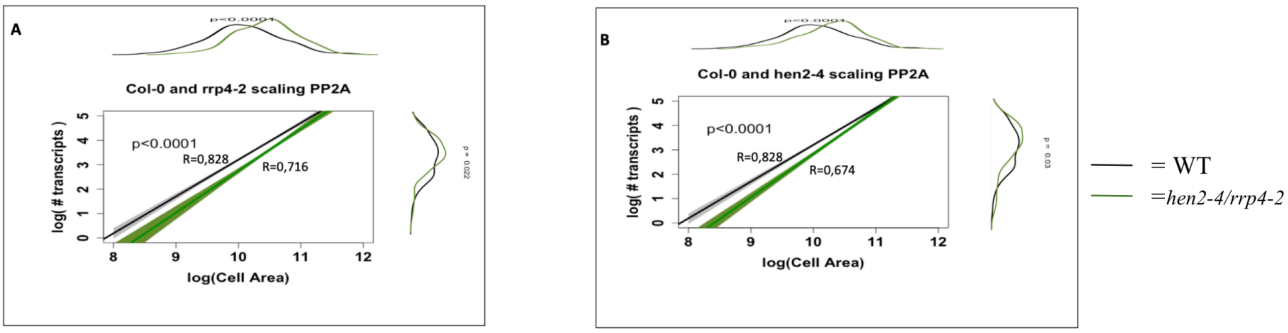

Figure 2. *hen2-4* and *rrp4-2* scale in a more pronounced way in PP2A compared to WT. The graph shows a comparison between the linear regressions of cell area and total number of transcripts for PP2A in *hen2-4* and *rrp4-2* mutants. The broader lines represent a 95% confidence interval for each value. R values for each regression model are indicated, and P values to compare both regression models. The density plots next to the Y and X axis of each plot represent the distribution of values for logarithmic transcripts (Y axis) and logarithmic area (X axis).

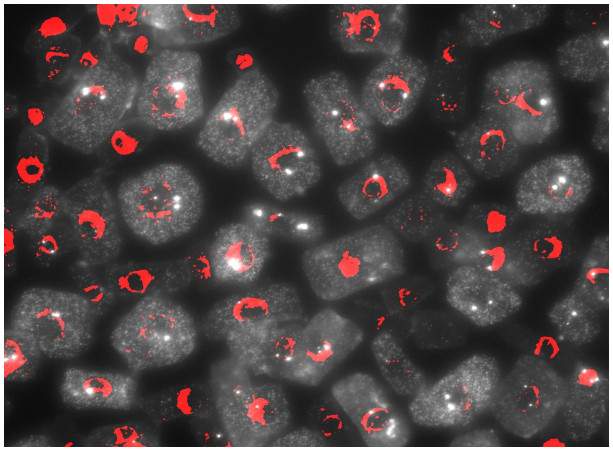

Col-0, NIA1

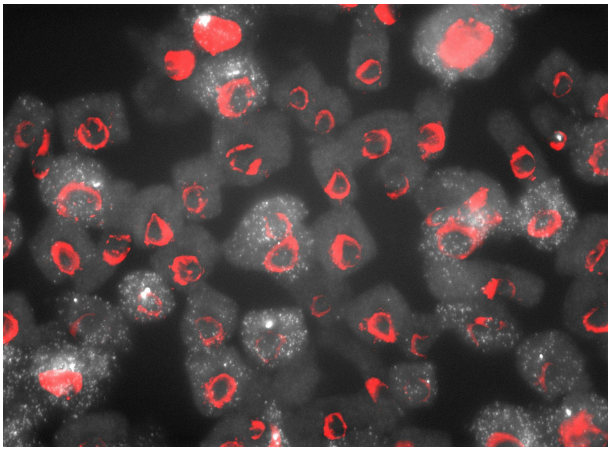

rrp4-2, NIA1

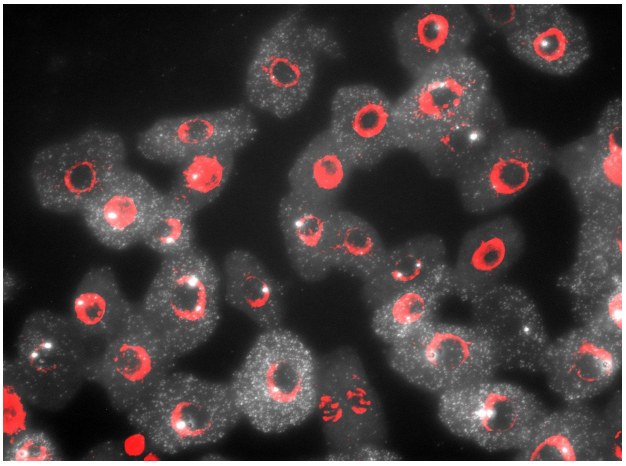

hen2-4, NIA1

Figure 3. Representative pictures of smFISH carried out on *hen2-4/rrp4-2* mutants and WT, showing NIA1 mRNA (magenta) and DAPI (red). Scale bars, 20µm.

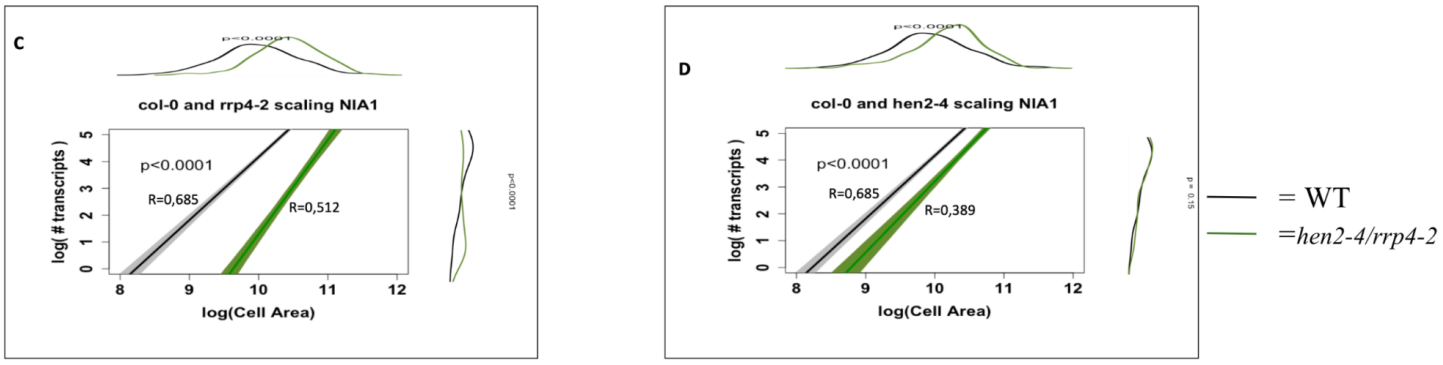

Figure 4. *hen2-4* and *rrp4-2* scale in a more pronounced way in NIA1 compared to WT. The graph shows a comparison between the linear regressions of cell area and total number of transcripts for NIA1 in *hen2-4* and *rrp4-2* mutants. The broader lines represent a 95% confidence interval for each value. R values for each regression model are indicated, and P values to compare both regression models. The density plots next to the Y and X axis of each plot represent the distribution of values for logarithmic transcripts (Y axis) and logarithmic area (X axis).

Kume *et al*. reported that the accumulation of mRNAs in the nucleus resulted in an increased N/C (nucleus/cell) ratio in fission yeast (Kume *et al*. 2017). Therefore, we wanted to test if sizes between cells and cellular compartments differed between *hen2-4*/*rrp4-2* mutants and WT. We performed variance analysis (ANOVA) in which the area of the cell, nucleus and cytoplasm for mutated genotypes and WT were quantified (*fig 5*). We also calculated the N/C ratios, and P values were determined to compare the ANOVA for each genotype. The cells of *hen2-4* and *rrp4-2* were larger than WT (P<0,001) - which might be a phenotype - but no difference was observed when comparing the N/C ratios (P>0,05).

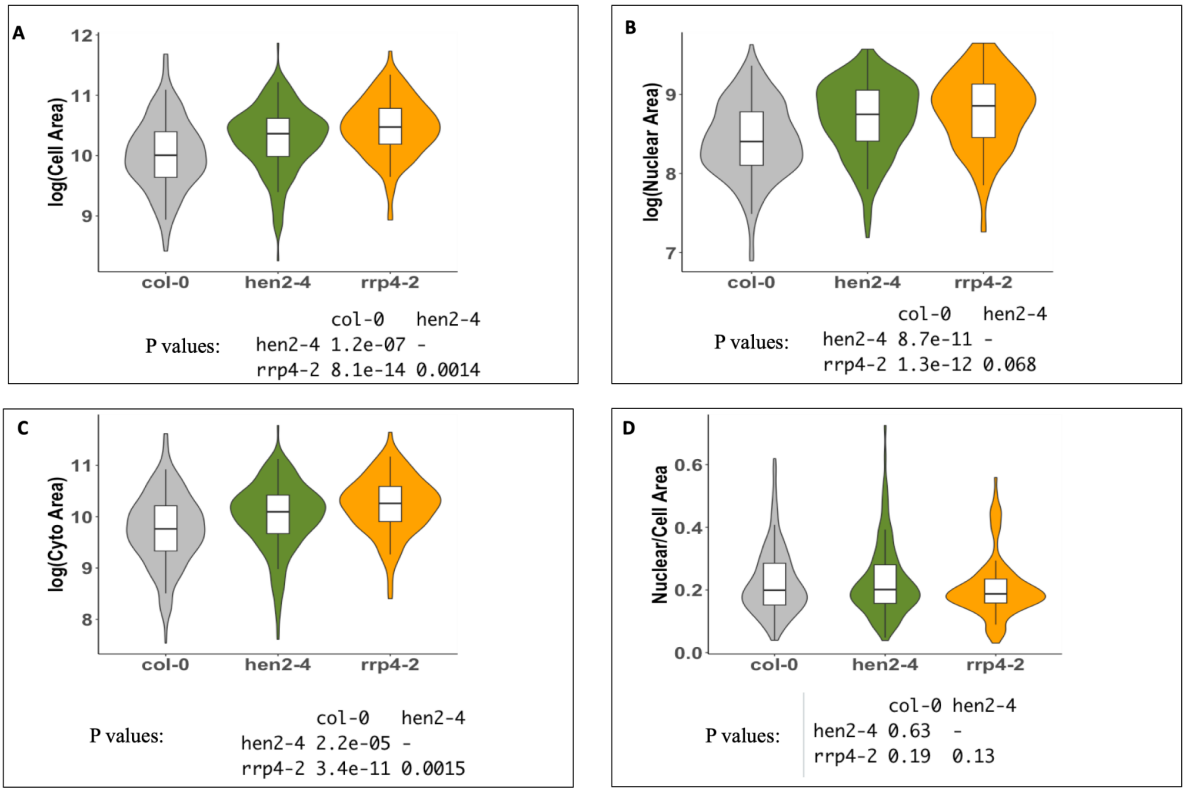

Figure 5. ***hen2-4* and *rrp4-2* have larger cells than WT, but the ratio between nuclear/cell area for mutants and WT show no difference**. Violin plots A, B and C show the area distribution of the cell/nucleus/cytoplasm of NIA1/PP2A in *hen2-4/rrp4-2* and WT - all of which were decided using ANOVA analysis. Grey color for WT, green for *hen2-4* and orange for *rrp4-2*. Violin plot D shows the ratio between nuclear/cell area for the mutants and WT. P values to compare each ANOVA analysis are indicated.

Considering *HEN2* and *RRP4* target the function of the nuclear exosome, we expected loss of these - hence disruption of exosome functionality - to result in accumulated transcripts in the nucleus. Therefore, we wanted to analyze the scaling on a nuclear level. This was also done by comparing linear regressions for *rrp4-2* and *hen2-4* mutants with WT, however this time with the following variables: Nuclear area vs nuclear transcripts; and cytoplasmic area vs cytoplasmic transcripts. Strikingly, the observed difference in scaling on a cellular level was not seen when comparing nuclear area with nuclear transcripts (P>0,05) (*fig 6*). Instead, the difference was seen when comparing cytoplasmic area with cytoplasmic transcripts (P<0,05) (*fig 7*), with the exception of NIA1 in *hen2-4* (P=0,099).

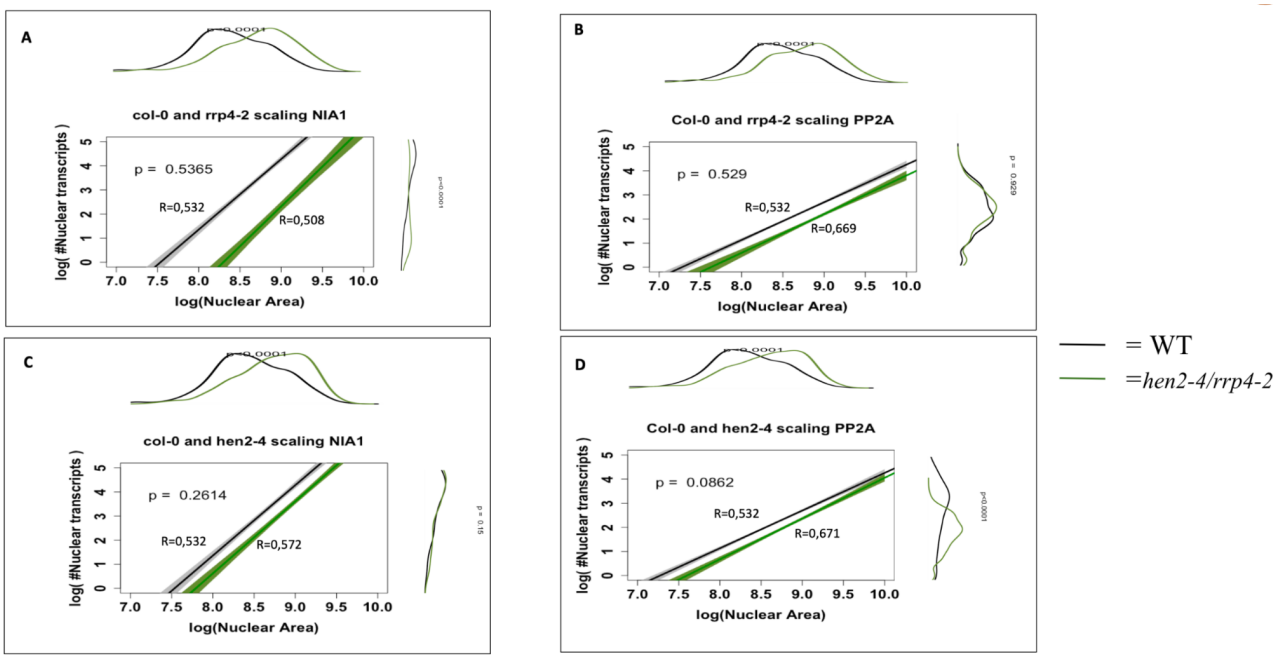

Figure 6. No difference in gene expression cell size scaling is observed at a nuclear level in *hen2-4* and *rrp4-2* compared to WT. The diagram shows a comparison between the linear regressions of nuclear area and nuclear transcripts for *NIA1* and *PP2A* in *hen2-4*/*rrp4-2* mutants compared to WT. The broader lines represent a 95% confidence interval for each value. R values for each regression model are indicated, and P values to compare both regression models. The density plots next to the Y and X axis of each plot represent the distribution of values for logarithmic transcripts (Y axis) and logarithmic area (X axis).

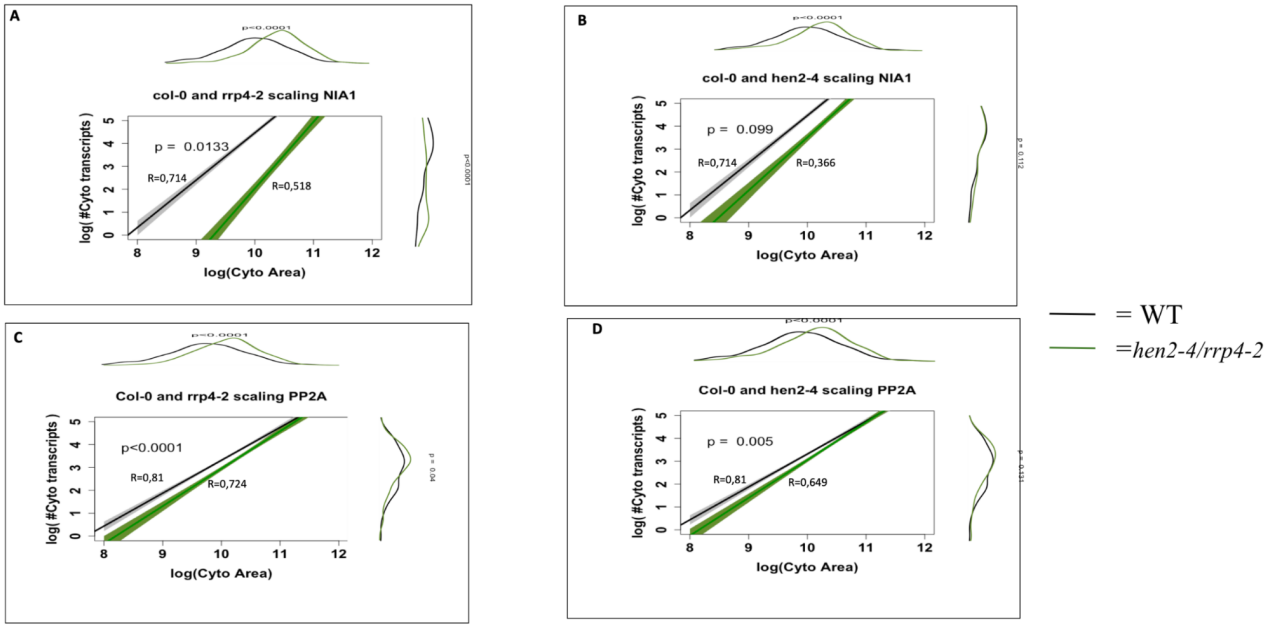

Figure 7. *rrp4-2* and *hen2-4* scale in a more pronounced way at a cytoplasmic level compared to WT. The diagram shows a comparison between the linear regressions of cytoplasmic area and cytoplasmic transcripts for NIA1/PP2A in *hen2-4* and *rrp4-2* mutants. The broader lines represent a 95% confidence interval for each value. R values for each regression model are indicated, and P values to compare both regression models. The density plots next to the Y and X axis of each plot represent the distribution of values for logarithmic transcripts (Y axis) and logarithmic area (X axis).

6: Discussion

In the present study, we show that cell size scaling of *A. thaliana* is altered in *hen2-4* and *rrp4-2* mutants. In general, *hen2-4* and *rrp4-2* accumulate transcripts in a more pronounced way with increasing cell size compared to WT. This indicates that in cells of *hen2-4* and *rrp4-2* - where the nuclear exosome is disrupted - gene expression cell size scaling is perturbed, suggesting a functioning nuclear exosome is crucial for maintaining mRNA homeostasis. Curiously, when looking at the number of transcripts within the nucleus only, no differences are observed between mutants and the wild type. Instead, the difference is observed in the cytoplasm. This could indicate that the cell compensates the increased accumulation of transcripts in the nucleus by increasing the export of transcripts to the cytoplasm. These findings suggest – similar to what has been reported in human cells – that the nuclear export machinery has an important function in plant gene expression cell size scaling (Berry *et al*. 2022b). Considering the export increases when exosome function is lost, one possibility could be that these two cellular functions are linked together, where loss of function for one is compensated by increased activity of the other. For future studies, it would be interesting to see how cell size scaling of *A.thaliana* is altered with mutations perturbing both nuclear exosome function and nuclear export.

smFISH is a highly effective method for enabling single cell quantification, something that previously has been restricted in plant transcription research (Duncan *et al*. 2018). Yet, for our purpose the method has a few restrictions. Because of high autofluorescence it has been optimized for *A. thaliana* root tips, and therefore only cells present in the root tip are studied (Rosa, 2023; Barrada *et al*. 2015). Thus, the root structure is not preserved and no information is provided regarding gene expression cell size scaling across cell types and tissues. Recently, Zhao *et al*. showed that whole-mount smFISH - an smFISH method where intact tissues are visualized - visualization of other tissues than the root tip is possible (Zhao *et al*. 2022). Finally, in smFISH experiments cells are fixed, meaning it does not reveal whether or how gene expression scaling varies over time.

Approximately 50 % of the *A. thaliana* genome is genetically redundant – meaning roughly half of the genes of *A.thaliana* have at least one paralog performing the same function (Cusack *et al*. 2021). In studies using a single gene knockout it is not uncommon that only a mild phenotype is observed when compared to WT, and that this phenotype becomes more

severe when using a higher-order mutant (Cusack *et al*. 2021). In our case, despite using single gene knockouts of *RRP4*, one subunit of *Exo9*, and the exosome cofactor *HEN2*, we still observed a phenotype strong enough to alter gene expression cell size scaling in A. *thaliana*, advocating our hypothesis about an mRNA based negative feedback mechanism - that in part and indirectly is controlled by the degradation of mRNA in the nucleus - operating in *A. thaliana*. To further develop this hypothesis, a next step could be exploring if an even stronger phenotype would be observed if using a higher-order mutant.

For the same purpose, gaining clarification in specifically how the synthesis of mRNA is affected by increased accumulation of transcripts in the nucleus could be important. In human cells synthesis of mRNA is reduced when levels of transcripts in the nucleus rise (Berry *et al*. 2022b). However - as shown here - for *rrp4-2* and *hen2-4* mutants in *A. thaliana*, the differences of the accumulation of transcripts between WT and mutants are observed in the cytoplasm. If the cell is increasing the export of transcripts to the cytoplasm upon reduction of mRNA decay in the nucleus, this might be to avoid accumulation of nuclear transcripts. One interpretation is - in line with our hypothesis about an mRNA negative feedback mechanism - that the cell is trying to reduce nuclear transcript accumulation in order to avoid inhibition of synthesis of new mRNAs. At this stage this interpretation is purely speculative, yet it could be an exciting starting point when formulating future experiments. A suggestion for such an experiment is performing smFISH with double mutants targeting both the nuclear exosome and the nuclear export machinery, and in addition using probes that target the introns rather than the exons. These probes would bind to nascent, unspliced mRNA, enabling quantification of newly synthesized transcripts, hopefully giving insight more specifically in how the synthesis of mRNAs is affected by accumulation of transcripts in the nucleus.

Table1. ***smFISH probe sequences used to detect PP2A transcripts. These probes were labelled with Quasar570.***

Probe nr	Probe Sequences (5'-3')
1	CCGAGCGATCTATCAATCAG
2	GACATCCTCACCAAAACTCA
3	TCGGGTATAAAGGCTCATCA
4	TAGCTCGTCGATAAGCACAG
5	CCAAGAGCACGAGCAATGAT
6	ATCAACTCTTTTCTTGTCCT
7	CATCGTCATTGTTCTCACTA
8	ATAGCCAAAAGCACCTCATC
9	ATACAGAATAAAACCCCCCA
10	CAAGTTTCCTCAACAGTGGA
11	TCATCTGAGCACCAATTCTA
12	TAGCCAGAGGAGTGAAATGC
13	CATTCACCAGCTGAAAGTCG
14	GGAAAATCCCACATGCTGAT
15	ATATTGATCTTAGCTCCGTC
16	ATTGGCATGTCATCTTGACA
17	AAATTAGTTGCTGCAGCTCT
18	GCTGATTCAATTGTAGCAGC
19	CCGAATCTTGATCATCTTGC
20	CAACCCTCAACAGCCAATAA
21	CTCCAACAATTTCCCAAGAG
22	CAACCATATAACGCACACGC
23	AGTAGACGAGCATATGCAGG
24	GAACTTCTGCCTCATTATCA

25	**CACAGGGAAGAATGTGCTGG**
26	**TGACGTGCTGAGAAGAGTCT**
27	**CCCATTATAACTGATGCCAA**
28	**TGGTTCACTTGGTCAAGTTT**
29	**TCTACAATGGCTGGCAGTAA**
30	**CGATTATAGCCAGACGTACT**
31	**GACTGGCCAACAAGGGAATA**
32	**CATCAAAGAAGCCTACACCT**
33	**TTGCATGCAAAGAGCACCAA**
34	**ACGGATTGAGTGAACCTTGT**
35	**CTTCAGATTGTTTGCAGCAG**
36	**GGACCAAACTCTTCAGCAAG**
37	**GGAACTATATGCTGCATTGC**
38	**GTGGGTTGTTAATCATCTCT**
39	**TGCACGAAGAATCGTCATCC**
40	**TTACTGGAGCGAGAAGCGAT**
41	**GAACATGTGATCTCGGATCC**
42	**CTCTGTCTTTAGATGCAGTT**
43	**CATCATTTTGGCCACGTTAA**
44	**CGTATCATGTTCTCCACAAC**
45	**ATCAACATCTGGGTCTTCAC**
46	**TTGGAGAGCTTGATTTGCGA**
47	**ACACAATTCGTTGCTGTCTT**
48	**CGCCCAACGAACAAATCACA**

Table2. ***smFISH probe sequences used to detect NIA1 transcripts. These probes were labelled with Quasar670.***

Probe nr	Probe Sequences (5'-3')
1	TGGTTTTGGTTTGGTTTGTG
2	ATAATGGCGGTTATCGACGG
3	GGTCGAATGAGCGAGGAGAA
4	ATGACGTCGAGAGTTTGGTT
5	GTGATGACTTCGGTTTCTTT
6	GAGTCGTCGTAACTGTCTAC
7	CAGCTCTTTGTAGTAAGGGA
8	GACGGTTCTAAATCGCTGTT
9	TTGAATCCAACTATCAGCCG
10	CGGCGTTGAATGGATGTTTT
11	GGAGTGATGAATCCATGGTG
12	ATTGACCAGTCTGACCAATT
13	CTGGGGAACTCGGAGATTAG
14	AGAGAAGTAGATACTCCGGC
15	CTCCTTCGAAGCAAACGTTT
16	CCTTCTTAATACTTGTTCCG
17	CATGATCCGGCGTTAAAAGC
18	ACAATGACCCGAACCGGAAA
19	TTGAGGCGTGACGATGATTC
20	AAAATCTCTGCGTGACCAGG
21	ACGGCTTCTGAGTAGTGAAT
22	CAGAAACACCAGCACCAGAA
23	TCTTTAGCACTGAGCAGATC

24	GGTTCCAGATGAGTTTATCA
25	GGTCGGGTGTTCGAAAACTA
26	GGAAATCTCAAGCTGACGCT
27	TTCGAGGCAGTGTTCATGAA
28	CAATCTGTACCTGCGTTTAT
29	CCAAAAGCTTCTTGGCTTTG
30	GTGATGAGTTCACCGATACG
31	CGTTAGGGGAAGAGTCGTAG
32	TTTGAGGCACCATGAACTGA
33	GGAGTTAGCTCTTTGATTGG
34	GGGTTGACCAAAGCAATGTT
35	TTACGAACGTCGTGCGAGAT
36	ACGGGTAAACCAAGCTGTTG
37	TCTGAGACAGAGTTTGTCGT
38	CCTTGGATGAACGTCTTTGA
39	TCATTGACCCGATTGGTAAC
40	CATTGCTAGTTTCTTGGCAA
41	AAGAATGTCATCCTCGGTTC
42	AAATCTTTAGCCTCTCCTTA
43	TTCCTTTGCGATTTCAACGA
44	CAGCTTCAGTTATAAACCCG
45	TAGATTTGGCTGCAACGCAA
46	TTAAGAGATCCTCCTTCACG
47	GTGCCCAAATAACCATGTAT
48	CATGAGTCCTGACATGCAAT

7: References

- Allmang C, Kufel J, Chanfreau G, Mitchell P, Tollervey D. (1999). Functions of the exosome in rRNA, snoRNA and snRNA synthesis. The EMBO journal, 18, 5399-5410. doi: 10.1093/emboj/18.19.5399
- Alvarez JM, Schinke AL, Brooks MD, Pasquino A, Leonelli L, Varala K, Safi A, Krouk G, Krapp A, Coruzzi GM. (2020). Transient genome-wide interactions of the master transcription factor NLP7 initiate a rapid nitrogen-response cascade. *Nat Commun*. Mar 2;11(1):1157. doi: 10.1038/s41467-020-14979-6.
- Barrada, Adam & Montane, Marie-Helene & Robaglia, Christophe & Menand, Benoît. (2015). Spatial Regulation of Root Growth: Placing the Plant TOR Pathway in a Developmental Perspective. *International journal of molecular sciences*. 16. 19671-97. doi: 10.3390/ijms160819671
- Berry S, Pelkmans L. (2022a). Mechanisms of cellular mRNA transcript homeostasis. *Trends in Cell Biology,* Vol. 32, No. 8. doi: 10.1016/j.tcb.2022.05.003
- Berry S, Muller M, Rai A, Pelkmans L. (2022b). Feedback from nuclear RNA on transcription promotes robust RNA concentration homeostasis in human cells. Cell Systems, 13, 454-470. doi: 10.1016/j.cels.2022.04.005
- Chekanova J, Gregory B, Reverdatto S, Chen H, Kumar R, Hooker T, Yazaki J, Li P, Skiba N, Penh Q, Alonso J, Brukhin V, Grossniklaus U, Ecker J, Belostotsky D. (2007). Genome-Wide High-Resolution Mapping of Exosome Substrates Reveals Hidden Features in the *Arabidopsis* Transcriptome. *Cell*, 131, 1340-1353. doi: 10.1016/j.cell.2007.10.056
- Cusack S, Wang P, Lotreck S, Moore B, Meng F, Conner J, Krysan P, Lehti-Shiu M, Shin-Han S. (2021). Predictive Models Of Genetic Redundancy in *Arabidopsis thaliana*. *Mol. Biol. Evol,* 38(8):3397-3414. doi:10.1093/molbev/msab111
- Duncan S, Rosa S. (2018). Gaining insight into plant gene transcription using smFISH. *TRANSCRIPTION*, 9, 166-170. doi: 10.1080/21541264.2017.1372043
- Justyna J. Olas & Vanessa Wahl. (2019). Tissue-specific *NIA1* and *NIA2* expression in *Arabidopsis thaliana*, Plant Signaling & Behavior, 14:11, doi: 10.1080/15592324.2019.1656035
- Duncan S, Olsson TSG, Hartley M, Dean C, Rosa S. (2017). Single Molecule RNA FISH in *Arabidopsis* Root Cells. *Bio Protoc*. Apr 20;7(8):e2240. doi: 10.21769/BioProtoc.2240
- Kamakura N, Otsuki H, Tsuzuki M, Takeda A, Watanabe Y. (2013). *Arabidopsis* AtRRP44A Is the Functional Homolog of Rrp44/Dis3, an Exosome Component, Is Essential for Viability and Is Required for RNA Processing and Degradation. PLoS ONE 8(11): e79219. doi:10.1371/journal.pone.0079219
- Kume K, Cantwell H, Neumann FR, Jones AW, Snijders AP, Nurse P. (2017). A systematic genomic screen implicates nucleocytoplasmic transport and membrane

growth in nuclear size control. *PLoS Genet* 13(5): e1006767. doi:10.1371/journal.pgen.1006767

- Lange H, Zuber H, Sement F, Chicher J, Kuhn L, Hammann P, Brunaud V, Bérard C, Boutellier N, Balzergue S, Aubourg S, Martin-Magniette M, Vaucheret H, Gagliardi D. (2014). The RNA Helicases AtMTR4 and HEN2 Target Specific Subsets of Nuclear Transcripts for Degradation by the Nuclear Exosome in *Arabidopsis thaliana*. *PLoS Genet* 10(8): e1004564. doi: 10.1371/journal.pgen.1004564
- Lange H, Gagliardi D. (2022). Catalytic activities, molecular connections, and biological functions of plant RNA exosome complexes. *THE PLANT CELL*, 34, 967-988. doi: 10.1093/plcell/koab310
- Letswaart R, Rosa S, Wu Z, Dean C, Howard M. (2017). Cell-Size-Dependent Transcription of FLC and Its Antisense Long Non-coding RNA COOLAIR Explain Cell-to-Cell Expression Variation. *Cell Systems* 4, 622-635. doi:10.1016/j.cels.2017.05.010
- Liu Q, Greimann J, Lima C. (2006). Reconstitution, activities, and structure of the eukaryotic RNA exosome. *Cell*, 127, 1223-1237. doi: 10.1016/j.cell.2006.10.037
- Mirth C, Frankino W, Shingleton A. (2016). Allometry and size control: What can studies of body size regulation teach us about the evolution of morphological scaling relationships? *Current opinion in Insect Science*, 93-98, 16. doi: 10.1016/j.cois.2016.02.010
- Mueller, F., Senecal, A., Tantale, K. *et al.* (2013). FISH-quant: automatic counting of transcripts in 3D FISH images. *Nat Methods* 10, 277–278. doi: 10.1038/nmeth.2406
- Olas, Justyna & Wahl, Vanessa. (2019). Tissue-specific NIA1 and NIA2 expression in Arabidopsis thaliana Tissue-specific NIA1 and NIA2 expression in Arabidopsis thaliana. *Plant Signaling & Behavior*. 14. doi: 10.1080/15592324.2019.1656035.
- Razavizadeh, R., Shojaie, B. & Komatsu, S. (2018). Characterization of *PP2A-A3* mRNA expression and growth patterns in *Arabidopsis thaliana* under drought stress and abscisic acid. *Physiol Mol Biol Plants* 24, 563–575. doi: 10.1007/s12298-018-0530-7
- Rosa, S. 2023. E-mail 10th of jan. < stefanie.rosa@slu.se >
- Sikorska, N., Zuber, H., Gobert, A. *et al.* (2017). RNA degradation by the plant RNA exosome involves both phosphorolytic and hydrolytic activities. *Nat Commun* 8, 2162. doi: 10.1038/s41467-017-02066-2
- Stringer C, Michaelos M, Pachitariu M. (2020). Cellpose: a generalist algorithm for cellular segmentation. *bioRxiv preprint*, doi: 10.1101/2020.02.02.931238
- Sun X, Bowman A, Priestman M, Bertaux F, Martinez-Segura A, Tang W, Whilding C, Dormann D, Shahrezaei V, Marguerat S. (2020). Size-Dependent Increase in RNA Polymerase II Initiation Rates Mediates Gene Expression Scaling with Cell Size. *Current Biology*. Volume 30, Issue 7, 1217-1230. doi: 10.1016/j.cub.2020.01.053
- Vargas-Garcia C, Ghusinga K, Singh A. (2018). Cell size control and gene expression homeostasis in single-cells. *Current Opinion in Systems Biology*, 8:109-116. doi: 10.1016/j.coisb.2018.01.002

- Western TL, Cheng Y, Liu J, Chen X. HUA ENHANCER2, a putative DExH-box RNA helicase, maintains homeotic B and C gene expression in Arabidopsis. (2002). Development. 129, 7, : 1569-81. doi: 10.1242/dev.129.7.1569
- Zhao L, Fonseca A, Meschichi A, Sicard A, Rosa S. (2022). Whole-mount smFISH allows combining RNA and protein 2 quantification at cellular and subcellular resolution. bioRxiv preprint. doi: 10.1101/2022.10.05.510616